

Predictive modelling of JET baseline scenarios from DTE2 towards DTE3

V.K. Zotta¹, L. Garzotti², S. Gabriellini¹, R. Gatto¹, C. Bourdelle³, C. Giroud², L. Frassinetti⁴, D. Frigione⁵, D.B. King², D.L. Keeling², D. Kos², M. Lennholm², K. Lawson², C. Leoni¹, P. Lomas², C. Lowry², S. Menmuir², G. Pucella⁶, F.G. Rimini², D. Van Eester⁷, S. Wiesen⁸, A. Kappatou⁹, N. Vianello¹⁰, M. Wischmeier⁹, JET Contributors* and the EUROfusion Tokamak Exploitation Team**

¹Dipartimento di Ingegneria Astronautica, Elettrica ed Energetica, Sapienza Università di Roma, via Eudossiana 18, 00184, Roma, Italy; ²United Kingdom Atomic Energy Authority, Culham Science Centre, Abingdon, Oxon, OX14 3DB, United Kingdom of Great Britain and Northern Ireland; ³CEA, IRFM, F-13108 Saint Paul Lez Durance, France; ⁴Fusion Plasma Physics, EECS, KTH Royal Institute of Technology, SE-10044 Stockholm, Sweden; ⁵University of Rome Tor Vergata, Via del Politecnico I, Rome, 00133, Italy; ⁶Dip.to Fusione e Tecnologie per la Sicurezza Nucleare, ENEA C. R. Frascati, via E. Fermi 45, 00044 Frascati (Roma), Italy; ⁷Laboratory for Plasma Physics, LPP-ERK/KMS, Bruxelles Belgium; ⁸DIFFER - Dutch Institute for Fundamental Energy Research, De Zaale 20, 5612 AJ Eindhoven, Netherlands; ⁹Max-Planck-Institut für Plasmaphysik, Garching, Germany; ¹⁰Consorzio RFX, Corso Stati Uniti, 4, Padova, 35127 Italy;

* See the author list of C.F. Maggi et al. 2024 Nucl. Fusion (<https://doi.org/10.1088/1741-4326/ad3e16>);

** See the author list of E.H. Joffrin et al 2024 Nucl. Fusion (<https://doi.org/10.1088/1741-4326/ad2be4>);

INTRODUCTION

The multi-year effort on the *Joint European Torus* (JET) for investigating key physics aspects of ITER operations has culminated with the last two deuterium-tritium (DT) experimental campaigns. While 2021 DT experiments (DTE2) focused mainly on the stationarity of the high fusion performance [1], 2023 D-T experiments (DTE3) aimed at the integration of reactor relevant scenarios in view of ITER and DEMO [2]. The high-current high-performance baseline scenario for DTE2 (from now on JET baseline scenario) has been successfully developed and sustained for 5 s in D, but when translated in T and DT it could not be sustained for more than 2-3 s [3]. The JET baseline scenario has been executed in DTE2 mainly at 3.5 MA and 3.3 T in presence of 50-50 DT beams using D pacing pellets. In DTE2, only two pulses were performed at 3.0 MA and 2.8 T with additional heating power $P_{aux} \approx 25$ MW. One of the two JET baseline pulses at 3.0 MA has been performed with neon (Ne) seeding aiming at demonstrating in DT the same beneficial effect of Ne on confinement demonstrated in D [4, 5, 6].

With Ne seeding, at lower plasma current (2.5 MA and 2.8 T), in a different divertor configuration and higher triangularity, the core-edge integrated scenario (from now on ITER baseline scenario) has been demonstrated for the first time in DTE2 [7]. However, the development of the ITER baseline scenario in DTE2 has been hindered by the constraints on the D-T neutral beam (NBI) heating power due to re-ionization heat load on limiters and duct pressure [7] found at higher fuelling rates. Both scenarios, JET and ITER baseline, have been successfully executed in DTE3 in presence of pure D-NBI, with an additional heating power $P_{aux} \geq 30$ MW, achieving good performance for at least 5 s [8].

In this contribution we investigate the fuel mix control in DT plasmas and how the 50-50 DT mixture is achieved through the balance of the different fuelling channels. Despite the relevance of fuel mix control for future fusion reactors, this topic is not often covered by integrated modelling due to the large uncertainties on particle sources from gas puffing in the edge region and in the scrape-off layer. However, progress has been made in the analysis and in the prediction of the last JET DT campaigns [9, 10, 11] and we are now presenting how, based on integrated modelling, a 50-50 DT JET baseline scenario has been achieved in presence of D-NBI. We present the validation done on DTE2 data, the blind predictions of the JET baseline scenario for DTE3 and the modelling results on actual DTE3 data for both scenarios.

INTEGRATED MODELLING OF DTE2 AND DTE3 PLASMAS

DTE2 has been preceded by a multi-year activity of predictive modelling [12] and it has been followed by an intense validation activity on multiple transport codes and first-principle

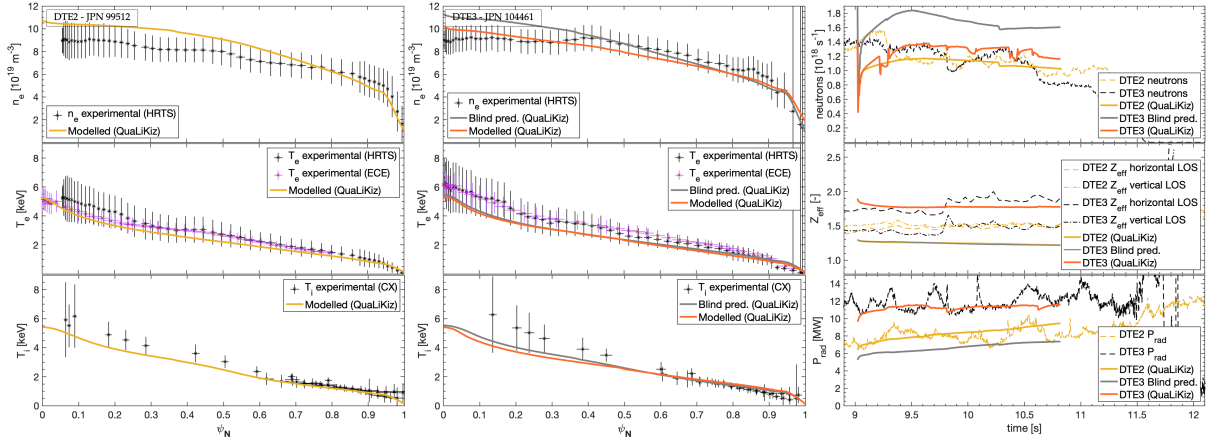


Figure 1: JET baseline scenario in DTE2 (JPN 99512) and DTE3 (JPN 104461), predicted plasma kinetic profiles compared with HRTS measurements for electron density and temperature, and with charge exchange spectroscopy for ion temperature. In the right-side panel, the neutron rate, the effective charge Z_{eff} and the bulk radiative power time traces are shown.

transport models [13]. In the framework of the modelling done in support of the JET baseline scenario for DTE2 [9, 10] we performed predictive simulations of the JPN 99512. For core transport modelling we use JINTRAC [14] equipped with the QuaLiKiz transport model [15] predicting the D and T densities, the electron and ion temperatures and the plasma current density profiles. ESCO is evolving the equilibrium consistently with the evolution of the plasma kinetic profiles, while the impurity density profiles (i.e. n_{Be} , n_{Ni} and n_{W}) are evolved with SANCO. The impurity mix composition is obtained constraining the Nickel content in the simulation to match the Ni radiative power estimated from the spectroscopy [16], the W content is adjusted to match the bulk radiative power and the Be content is adjusted to reach the measurement of the effective charge Z_{eff} . PENCIL and PION are used for the determination of the heating deposition profiles, FRANTIC for the computation of the ionization sources. Since the boundary conditions are imposed at the separatrix, where we assumed $T_e = T_i = 100$ eV, the pedestal is modelled with ELM average transport coefficients. The determination of the ELM averaged transport coefficients is obtained scanning the thermal diffusivity χ and the particle diffusivity D to reproduce the experimental pedestal top and tuning the particle sources of the main ion species. To validate the modelling settings, we performed the predictive simulation of the DTE2 pulse JPN 99512 achieving a good agreement with the experimental data shown in Fig. 1. Starting from the results of the DTE2 predictive modelling, we increased the additional heating power in the simulation up to $P_{\text{NBI}} = 30$ MW and we

Table 1 Main plasma parameters of the modelled pulses.

JET pulse number	99512	104461	104623
Baseline Scenario	JET DTE2	JET DTE3	ITER DTE3
Simulated time window [s]	9.0 - 10.8	9.0 - 10.8	12.5 - 13.6
T concentration [%]	50	49	52
B_t [T]	2.8	2.8	2.7
I_p [MA]	3.0	3.0	3.0
q_{95}	3.3	3.2	2.6
D gas [10^{22} s^{-1}]	0	0	2.8
T gas [10^{22} s^{-1}]	0.72	0.87	2.2
S_{pel} [10^{22} s^{-1}]	0.6 (D)	0.52 (D)	0
β_N	1.9	2.1	1.5
P_{NBI} [MW]	23.7	28.7	24.8
P_{ICRH} [MW]	1.8	3.8	2.9
P_{RAD} [MW]	8.1	11.8	6.6
$n_{e,0}$ [10^{19} m^{-3}]	9.1	8.7	12.3
$\langle n_e \rangle$ [10^{19} m^{-3}]	6.2	6.4	10.8
$T_{e,0}$ [keV]	5.2	6.4	3.1
$\langle T_e \rangle$ [keV]	2.1	2.1	1.2
$T_{i,0}$ [keV]	5.2	5.7	2.8
W_{th} [MJ]	7.7	8.5	5.5
neutron rate [10^{16} s^{-1}]	117.4	118.9	36.9
Z_{eff}	1.5	1.7	1.4

Since the boundary conditions are imposed at the separatrix, where we assumed $T_e = T_i = 100$ eV, the pedestal is modelled with ELM average transport coefficients. The determination of the ELM averaged transport coefficients is obtained scanning the thermal diffusivity χ and the particle diffusivity D to reproduce the experimental pedestal top and tuning the particle sources of the main ion species. To validate the modelling settings, we performed the predictive simulation of the DTE2 pulse JPN 99512 achieving a good agreement with the experimental data shown in Fig. 1. Starting from the results of the DTE2 predictive modelling, we increased the additional heating power in the simulation up to $P_{\text{NBI}} = 30$ MW and we

changed the NBI gas from DT to D. The T gas puff has been increased in the “blind” prediction of about 20% to balance the presence of D-NBI on the main ion plasma composition. Using the increase of T gas puff inferred by integrated modelling, the fueling recipe for DTE3 has been established and the JPN 104461 has been executed achieving a 50-50 DT mixture. The main differences between the two JET baseline pulses concern the impurity mix compositions and the increased auxiliary heating power of about ~ 5 MW of NBI and ~ 2 MW of ICRH. The presence of a higher impurity content in DTE3 is highlighted by a higher Z_{eff} (increasing from 1.5 to 1.8) and by an increase in the bulk radiative power. The results of the blind prediction compared with the modelling on actual DTE3 data are shown in Fig. 1. It is worth noting that the predicted performance for DTE3 is 40% higher than what achieved in the experiment. This discrepancy has been extensively studied iterating JINTRAC predictive simulations with TRANSP interpretative analysis [17] investigating the role of impurity mix composition, main ion plasma composition and anomalous fast ion diffusion. Both TRANSP interpretative and JINTRAC predictive analysis, show that the discrepancy can be consistent with: i) an impurity composition with higher Be dilution with respect to DTE2; ii) a decrease of T concentration towards the magnetic axis; and iii) an anomalous fast ion diffusion in the order of $0.5 \text{ m}^2/\text{s}$ [17]. In the JINTRAC predictive modelling on actual DTE3 data (orange in Fig. 1), we’ve been able to reproduce the experimental neutron yield only deactivating the *ad-hoc* electromagnetic stabilization [18] of ITG mode in QuaLiKiz. This is currently under investigation as the *ad-hoc* electromagnetic stabilization has been extensively used in previous JINTRAC-QuaLiKiz modelling for the JET baseline scenario in D, and DT [9, 10]. Moreover, the JPN 104461 shows a higher β_N due to the increased additional heating power and has been stopped earlier by the intervention of real-time controls for the presence of MHD instabilities.

With a similar approach we modelled the unseeded ITER baseline pulse JPN 104623. The ITER baseline is characterized by vertical-vertical divertor configuration (corner-corner in the JET baseline) and a higher nominal gas puff $\Gamma_{nom} \approx 5 \cdot 10^{22} \text{ s}^{-1}$ without pellets. In the ITER baseline the gas is mainly injected from the divertor with only a 30% of the nominal gas puffing rate injected from the top of the main chamber, while in the JET baseline the gas puffing is performed from the top and from the mid plane of the main chamber. The significantly higher gas injection in the ITER baseline pulse produces a higher electron density profile with a density at the top of the pedestal $n_{e,ped}(\text{ITER-b}) > 2 \cdot n_{e,ped}(\text{JET-b})$ and lower electron and ion temperatures. Because the higher density, the ITER baseline shows a lower P_{rad} and a lower Z_{eff} , with respect to the JET baseline, indicating a lower impurity content. The simulated plasma profiles are in agreement with the measurements as well as the neutron yield (Fig. 2), with the QuaLiKiz *ad-hoc* electromagnetic stabilization included in the predictive simulation.

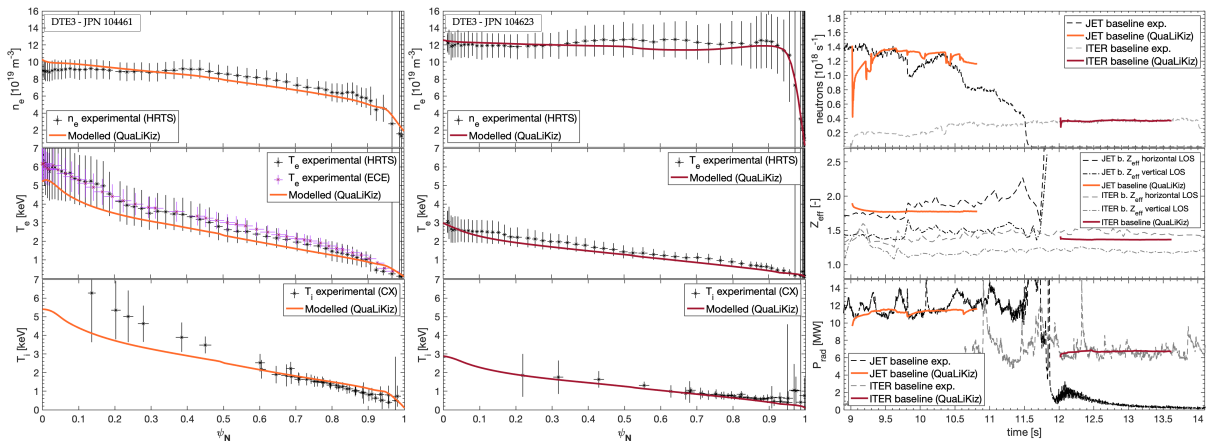


Figure 2: JET baseline and ITER baseline scenarios in DTE3, predicted plasma kinetic profiles compared with HRTS measurements for electron density and temperature, and with charge exchange spectroscopy for ion temperature. In the right-side panel, time traces of the neutron rate, of the effective charge Z_{eff} and of the bulk radiative power are shown.

DISCUSSION

We have presented the first results of the predictive modelling performed with JINTRAC on DTE3 data for the two scenarios featuring high current, the JET baseline and the ITER baseline. The experimental fuel mix of the JET baseline scenario has been achieved following the indications from the integrated modelling, performed before the campaign, leading to a T nominal fuelling ratio $T/(D+T) \approx 63\%$ while in the simulations the T/(D+T) ionization sources ratio results 50%. The ITER baseline unseeded pulse, in a different divertor configuration and with a different location of the gas puffing, has a significantly higher nominal gas rate with a nominal fuelling ratio $T/(D+T) \approx 44\%$, while in the simulations the T/(D+T) ratio of ionization sources is 59%. In the JET baseline scenario, the difference between the nominal fuelling ratio and the ratio of the ionization sources in the modelling can be attributed to the increased fuelling efficiency of D injection through pellets. For the ITER baseline scenario, the significant difference of the nominal experimental sources with respect to the ionization sources found in the integrated modelling needs to be further investigated. In this scenario, it could be related to a difference in the fuelling efficiency of the two hydrogen isotopes. In this context, the integration of the Scrape-off layer in the simulation domain, with a similar framework presented in [11] for the DTE2 JET baseline, could help clarifying the impact of the gas puffing location on the fuelling efficiency. Further studies will investigate the impact of the D-NBI fuelling on the T core concentration profile including the effect of the *ad-hoc* electromagnetic stabilization. In DTE3, the ITER baseline scenario with Neon seeding has achieved low divertor target temperatures with partial divertor detachment [8]. The Neon seeding allows the access to a regime characterized by lower densities at the edge [19], with respect to the unseeded pulse presented in this contribution, with a fusion performance that slightly exceeds the fusion performance achieved by the JET baseline scenario in DTE3.

The JET baseline scenario development at 3.0 MA has been limited in time in DTE3 and the presence of MHD instabilities has limited the fusion performance of the JET baseline pulses. However, a first DT JET baseline pulse has been sustained for 5 s at 3.0 MA with reduced NBI power ($P_{\text{NBI}} \approx 27$ MW) and is now under analysis. Lastly, the limitation on auxiliary heating power, due to MHD activity in DT 3.0 MA pulses, confirms that the choice of operating at higher plasma current (3.5 MA / 3.3 T), with higher densities, would have been the most promising path for pursuing high fusion performance in DT in the JET baseline scenario.

Acknowledgements This work has been carried out within the framework of the EUROfusion Consortium, funded by the European Union via the Euratom Research and Training Programme (Grant Agreement No 101052200 - EUROfusion). Views and opinions expressed are however those of the author(s) only and do not necessarily reflect those of the European Union or the European Commission. Neither the European Union nor the European Commission can be held responsible for them.

We acknowledge financial support under the National Recovery and Resilience Plan (NRRP), Mission 4, Component 2, Investment 1.1, Call for tender No. 104 published on 2.2.2022 by the Italian Ministry of University and Research (MUR), funded by the European Union – NextGenerationEU – Project Title “Fusion-fission hybrid pilot reactors for sustainable energy transition” – CUP B53D23005060006.

References

- [1] C.F. Maggi *et al* 2024 *Nucl. Fusion* (<https://doi.org/10.1088/1741-4326/ad3e16>)
- [2] A. Kappatou, *this conference*
- [3] L. Garzotti *et al* at IAEA FEC 2023
- [4] C. Giroud *et al* at IAEA FEC 2021
- [5] S. Gabriellini *et al.* 2023 *Nucl. Fusion* **63** 086025
- [6] M. Marin *et al*, 2023 *Nucl. Fusion* **63** 016019
- [7] C. Giroud *et al* at IAEA FEC 2023
- [8] C. Giroud *et al* at 26th PSI Conference 2024
- [9] V.K. Zotta *et al* 2022 *Nucl. Fusion* **62** 076024
- [10] V.K. Zotta *et al* 2022 at 48th EPS Conf. on Plasma Physics
- [11] C. Leoni *et al.*, *this conference*
- [12] J. Garcia *et al* 2023 *Nucl. Fusion* **63** 112003
- [13] H.-T. Kim *et al* 2023 *Nucl. Fusion* **63** 112004
- [14] M. Romanelli *et al* 2014 *Plasma Fusion Res.* **9** 3403023
- [15] C. Bourdelle *et al* 2016 *Plasma Phys. Control. Fusion* **58** 014036
- [16] A. Czarnecka *et al* 2011 *Plasma Phys. Control. Fusion* **53** 035009
- [17] J. Lombardo *et al.*, *this conference*
- [18] F.J. Casson *et al* 2020 *Nucl. Fusion* **60** 066029
- [19] I.S. Carvalho *et al.*, *this conference*